PAPER

A large-scale pico-droplet array for viable bacteria digital counting and dynamic tracking based on a thermosetting oil†

Yuanjie Suo,[a] Weihong Yin,[b] Wenshuai Wu,[b] Wenjian Cao,[a] Qiangyuan Zhu ✶[a] and Ying Mu ✶[a]

The rapid and accurate detection of viable bacteria is of great importance in food quality monitoring and clinical diagnosis. *Escherichia coli* (*E. coli*) is a major pathogenic bacterium, which causes potential threats to food safety and human health. Therefore, rapid and portable methods for preventing *E. coli* outbreaks are needed. Single cell analysis can be performed at the single-cell level, which has great advantages for analysis and diagnosis. Herein, we employed a thermosetting oil to generate a large-scale pico-droplet array for viable bacteria digital counting and dynamic tracking. In this array, the droplets can be solidified without any inducers due to the cross-linking reaction of the hydrosilation of vinyl silicone oil and hydrosilicone oil. Single *E. coli* cells were encapsulated in solidified droplets to form a microcolony. Resazurin was used as a fluorescent indicator to achieve amplification of bacterial growth signals. This method can achieve digital counting of viable *E. coli* cells in 4 h. We achieved real-time monitoring of *E. coli* cell growth and division in droplets. It is rapid, simple, and does not require a pre-enrichment process when compared to the traditional plate counting method. We successfully applied the method for the enumeration of *E. coli* in milk. In conclusion, the thermosetting oil enables the immobilization of droplets to achieve real-time monitoring and digital counting of bacterial growth without impairing the flexibility of droplet microfluidics, and it has the potential to provide dynamic information at high resolution in this process.

1. Introduction

Foodborne pathogens pose a major threat of infectious life-threatening diseases all around the world. *Escherichia coli* O157:H7 (*E. coli* O157:H7) is a Gram-negative, rod-shaped, facultative anaerobic foodborne pathogen.[1] *E. coli* O157:H7 is regarded as one of the most prevalent foodborne pathogens,[2] which can cause life-threatening diseases such as bloody diarrhea, kidney failure and death.[3,4] It can spread through various foods and drinking water, and can cause infection even at low concentrations. In March 2018, an outbreak caused by *E. coli* O157:H7 *via* food samples occurred in the US, resulting in 210 cases of disease and 5 deaths.[5,6] In 2014, according to the European Food Safety Authority, *E. coli* O157:H7 caused 2741 cases of foodborne diseases in Europe.[7] Therefore, the rapid and precise quantification of viable bacteria in food and clinical infectious samples plays a key role in food safety and diagnosis of bacterial infection.[8]

Plate counting is a representative method for quantifying viable bacteria. However, this method is based on the traditional cell culturing process which is labor-intensive and time-consuming.[9–11] It often requires more than 24 h for sufficient microbial growth, limiting its application in rapid bacterial enumeration. Another popular method for determining microbial concentrations is microscopy as it can enable the direct and rapid counting of the total number of bacteria. But the high requirement of microscopy and the small vision of the observation field limit its application in relatively high bacterial samples.[12] Nevertheless, one of the most important advantages of these two methods is that they can count viable bacteria when compared with the method based on nucleic acids, which is of great significance for food and clinical samples. As such, highly simple, fast and precise counting tools to screen viable pathogens are required.

To date, droplet-based microfluidics has rapidly emerged as one of the key technologies, opening up a new avenue of

a Research Centre for Analytical Instrumentation, Institute of Cyber-Systems and Control, State Key Laboratory of Industrial Control Technology, Zhejiang University, Hangzhou, Zhejiang Province, 310027, PR China. E-mail: qyzhu2008@zju.edu.cn, muying@zju.edu.cn

b College of Life Sciences, Zhejiang University, Hangzhou, Zhejiang Province, 310058, PR China

†Electronic supplementary information (ESI) available. See DOI: https://doi.org/10.1039/d2an00680d

possibilities in microbiology.[13] Droplet-based microfluidic devices can rapidly generate and manipulate nanoliter or sub-nanoliter droplets within microchannel environments.[14,15] Individual droplets make it possible for single cell dispersion based on stochastic confinement.[16,17] Such single cell dispersions are conducive to the cultivation of single cells and provide a direction for the development of quantification of viable bacteria. However, conventional droplets stabilized with surface tension may undergo unwanted fusion and fission under some conditions,[18–20] especially when the droplets are transferred to the incubation tubes and imaging chambers.[21,22] Besides, droplet-to-droplet coalescence may occur if they come into contact with each other[22] during the heating process, which may affect the accuracy of quantification.[23] In addition, the imaging readout of the whole droplets can be achieved by using the planar droplet array but the free motion of droplets usually makes it difficult, especially in the case of real-time monitoring.[24]

A stable, spatially defined droplet array technology has been developed to address the limitations of the conventional droplet array. It has great advantages in monitoring, identifying and indexing individual droplets for single cell analysis.[25,26] Individual droplets can be monitored by storing them in microwells,[27] dropspots,[28,29] or capture structures[25] to obtain time-resolved information. Each of these methods has certain advantages, though all have some limitations as well. These structures limit the parameters of droplet generation (e.g., flow rate, droplet size, and generation frequency), which hinders the tight arrangement of droplets and thereby compromises the flexibility and throughput of droplet microfluidics.

To overcome the limitations of the aforementioned methods and accomplish real-time monitoring of individual droplets for dynamic bacterial growth analysis, a thermosetting oil and fluorescence imaging based planar droplet array system was developed herein. In this device, the thermosetting oil can immobilize droplets by transforming them into elastic solids after droplet generation based on previous work from our group.[30] The oil phase consists of 10 cSt silicone oil, nonionic surfactant (5225C formulation aid), vinyl silicone oil with a high vinyl content (double-19), vinyl silicone oil with a high degree of polymerization (RTV-615A), hydrosilicone oil (RTV-615B), and a platinum catalyst. It is endowed with biocompatibility and air permeability. The curing process is based on the hydrosilylation of vinyl silicone oil and hydrosilicone oil, which can be accelerated spontaneously in the presence of the Pt catalyst. This process does not require other inducers (e.g., UV[31] or charged ions[32]), thus reducing the damage to bacterial cells. We employed resazurin as an indicator to achieve the resazurin-amplified fluorescence detection of E. coli at the single cell level in the chip array. The bacterial suspension with a specific medium and resazurin was encapsulated in pico-liter droplets. The proliferation of single cells in pico-droplets could translate resazurin molecules into strongly fluorescent resorufin molecules as oxidation–reduction indicators in response to cellular metabolic activity.[33,34] This strategy provides an effective substitute for detecting the "microcolonies" proliferating from individual bacteria within pico-droplets. After a few hours of cultivation, positive droplets containing viable cells can be distinguished from negative droplets, showing that the thermosetting oil and fluorescence imaging based dynamic bacteria growth analysis could be a reliable approach in the research of viable bacterial counting and tracking. More importantly, the thermosetting oil developed in this work ensures the stability of the droplets and provides an efficient strategy for single cell monitoring without any pretreatment process.

2. Materials and methods

2.1. Materials and apparatus

10 cSt silicone oil (PMX-200) and 5225C formulation aid were purchased from Dow Chemical (Auburn, MI, USA). Double-19 was obtained from Guiyou New Material Technology (Shanghai, China). Double-19 was obtained from Guiyou New Material Technology (Shanghai, China). RTV615-A and -B were purchased from Momentive Performance Materials (Waterford, NY). Resazurin was purchased from Sigma-Aldrich Inc. (USA). Cell culture medium was purchased from Qingdao Haibo Biotechnology Co., Ltd (Qingdao, China).

Two syringe pumps (Pump 11 Elite, Harvard Apparatus) were used to generate droplets in the microfluidic chip. An inverted fluorescence microscope (IX83, Olympus, Japan) equipped with a CMOS camera (Prime, Teledyne Photometrics, USA.) was employed for fluorescence imaging.

2.2. Measurement of thermosetting oil properties

The mixed oil was composed of 51.2 wt% silicone oil (10 cSt), 10.5 wt% 5225C formulation aid, 18.1 wt% double-19, 8.3 wt% RTVA, 9.9 wt% RTV-B, and 2 wt% Pt catalyst.

The mixed oil was placed at different temperatures to observe its solidification state at different temperatures. The mixed oil was divided into five groups, and each group was placed at 25 °C, 37 °C and 95 °C respectively, for continuous observation.

2.3. Cell culture and preparation of artificially contaminated samples

E. coli (ATCC 25922) was obtained from American Type Culture Collection (ATCC). The strain was cultured in Luria–Bertani (LB) broth at 37 °C for 18 h. Following the incubation, 8 mL of the enriched culture was pooled into sterile centrifuge tubes and centrifuged at 3000 rpm at 25 °C for 10 min. The cell pellets were suspended in sterile normal saline (0.85% NaCl) and the OD 600 value was adjusted to ~1.0 (corresponding to ~1×10^9 CFU mL^{-1}). Then a series of dilutions were performed to obtain concentrations ranging from 10^1 to 10^7 CFU mL^{-1}. The final bacterial concentration was determined by the plate counting method. The final samples were composed of 150 μL (1 mg mL^{-1}) of resazurin, 100 μL of bacterial dispersion and 750 μL of mEC solution. All bacterial samples were prepared and used immediately in experiments.

2.4. Chip design and fabrication

Flow-focusing droplet microfluidic chips were produced using soft lithography techniques. First, the silicon wafer was cleaned and heated at 200 °C for 15 min to completely remove the surface moisture. Next, a 50 μm-thick layer of SU-8 3050 was coated onto the silicon wafer with a spin-coater. The coated silicon wafer was placed on a program-controlled temperature plate, heated at 95 °C for 30 min, and cooled at room temperature. The composite unit was exposed for 6 s using a UV exposure machine through a photolithography mask. Then, a two-step, post-exposure baking process (65 °C for 1 min and 95 °C for 5 min) was performed. Finally, the silicon wafer was developed and baked at 200 °C for 30 min.

For the chip based on the thermosetting oil, a total of 6 g of PDMS (A : B/10 : 1) was poured onto the centre of the mold, degassed in a vacuum chamber for 30 s and subjected to spin-coating (200 rpm for 30 s) to form a thin film of 400 μm. After baking at 85 °C for 30 min, the film was carefully peeled off from the mold and cut as required. A blank PDMS as a temporary layer was placed on the droplet storage zone to prevent it from being activated by plasma. Two blank PDMS adaptors (5 mm thick), as the inlet/outlet holders for the tube connection, were attached to the upper surface of the PDMS film. Then the PDMS film supported by the blank PDMS layer and two adaptors was bound to a clean glass slide after plasma treatment. After that, the temporary PDMS layer was removed and a PCR sealing film was attached over the droplet storage zone (Fig. S1†).

2.5. Droplet generation and single cell incubation

The bacteria samples containing mEC broth, resazurin, and *E. coli* at predetermined concentrations were prepared before each experiment to serve as an aqueous phase. The cell suspension was injected into the microfluidic devices by a syringe pump at a flow rate of 40 μL h^{-1}. The developed oil was used to generate single-cell emulsions at a flow rate of 80 μL h^{-1}. The droplets were stored in the accommodation chamber to form a monolayer droplet array. After being filled with single-cell droplets, the chips were enclosed by loading a mixture of PDMS and the Pt catalyst into microchannels from the inlets and outlets. Then the chips were placed in a humid incubator, which can provide a humid environment to avoid evaporation. The chips were incubated at 37 °C for 5 h to facilitate bacterial replication. The droplet array was examined and the fluorescence images were captured every 1 h with an inverted microscope (IX83, Olympus).

2.6. *E. coli* detection in milk samples

Milk samples were purchased from a local supermarket. Artificially contaminated samples were injected into the microfluidics for droplet generation and cultivation. Then the fluorescence signal of droplets was analyzed. Each sample was quantified by at least three repeats. Spiked samples were also cultured in parallel with LB agar plates for cell counting as control.

2.7. Data acquisition and analysis

After incubation, the fluorescence images of chips were acquired using an inverted fluorescence microscope (IX83, Olympus, Japan) equipped with a CMOS camera (Prime, Teledyne Photometrics, USA.). The images of compressed droplets in the chip were analyzed with Image J to measure the precise diameter. Data acquisition from fluorescence images and downstream data analysis were performed on Image J and Origin 8.0 pro.

3. Results and discussion

Droplet microfluidics provides a reliable and promising technology platform for biological applications. The real-time growth monitoring and tracking of bacteria at the single cell level is of great significance for follow-up bacterial research. The main purpose of this work is to design a droplet microfluidic chip based on a thermosetting oil for real-time growth monitoring and tracking of bacteria at the single cell level. At the same time, the growth signal of bacteria is transformed into a fluorescence signal by using resazurin as an indicator. The overview scheme is shown in Fig. 1.

3.1. Design and fabrication of the microfluidic chip

The schematic of the droplet chip is shown in Fig. 2 and Fig. S2.† It uses a flow-focusing configuration to generate the droplets. The chip contains one fission structure and two ramification regions, which is convenient for adjusting the size of droplets and making a more uniform distribution of droplets inside the storage chamber. This structure also increases the generation rate of droplets. The chip consists of four layers, including a bottom glass slide, a thin PDMS layer with a droplet channel above the glass, two PDMS adaptors of droplet inlet and outlet, and a PCR sealing film on the top. The major advantage of this design is to solve the problem of droplet evaporation. As is well-known, the PDMS material is gas permeable,[35] which makes cell cultivation possible in the PDMS chamber by supplying sufficient air.[36] However, its permeability also leads to serious water evaporation problems, especially when heated.[37] For bacteria, whether it needs oxygen to grow depends on the type of the bacteria. *E. coli* is a facultative anaerobic microorganism. It can grow in droplets which have limited nutrient supply as well as a low level of oxygen. Therefore, when using the droplet chip to culture *E. coli* cells, the evaporation problem caused by air permeability should be considered first. Some studies have introduced extra water channels as a sacrificial layer to avoid evaporation.[38] A thin film of Parylene C[39] or fluorosilane polymer[40] has also been used as a water vapor barrier in the integrated fluidic chips. However, these operations make chip processing time-consuming and laborious. In this study, we employ the sandwich multilayer chip with a water incubator to solve this problem. Herein, the attachment of a commercially available adhesive PCR sealing film on the top, simplifying the proces-
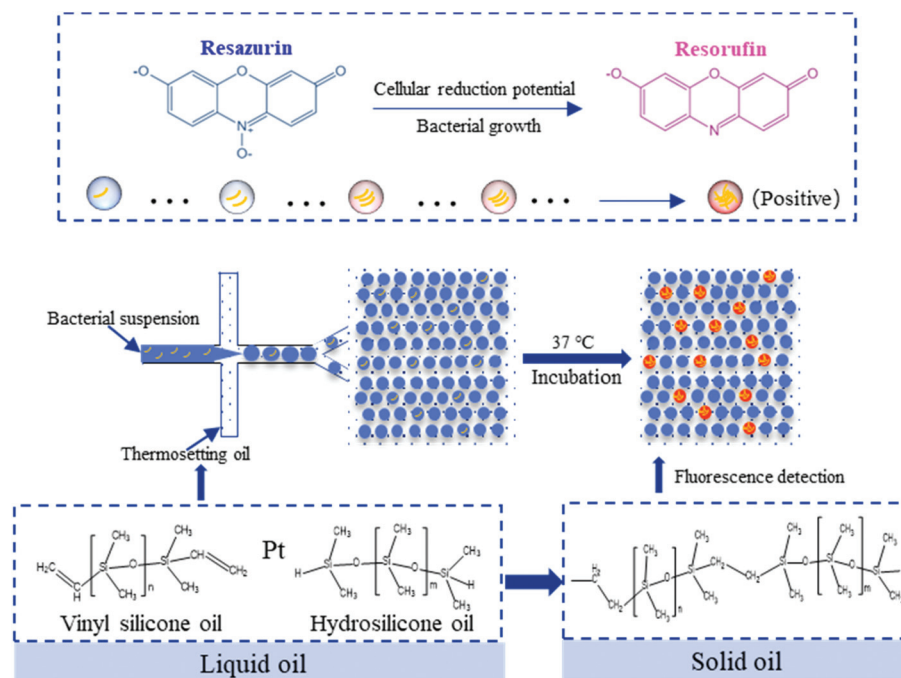
Fig. 1 Schematic illustration of single bacterial cell dynamic growth in the droplet array immobilized by the thermosetting oil.

sing of the chip, can prevent water evaporation to a certain extent when compared with previous anti-evaporation designs. Before the droplet generation and bacterial growth analysis, the chip was placed in a humid environment and incubated at 37 °C overnight. During this step, the chip can adapt to the incubation environment in advance, so as to prevent the loss of water in the subsequent reaction.

3.2. Properties and stability of the thermosetting oil-based droplets

Since the thermosetting oil can be transformed from the liquid state to the solid state without any inducer, it is suitable for droplet generation and immobilization. The thermosetting oil was first developed by our group.[30] The stability of the oil depends on the proportions of the components. In order to generate smaller size droplets in a stable state, we made a minor modification to the portions of the component of the oil when compared to the previous work. In this work, the thermosetting oil consisted of 51.2 wt% silicone oil (10 cSt), 10.5 wt% 5225C formulation acid, 18.1 wt% double-19, 8.3 wt% RTVA, 9.9 wt% RTV-B, and 2 wt% Pt catalyst. 10 cst silicone oil reduces the viscosity of the mixture oil. As an interface stabilization agent, the 5225C formulation acid helps to form monodisperse emulsions and stabilize droplets before oil solidification. The main principle of the thermosetting oil is the hydrosilylation reaction of vinyl silicone oil and hydrogen silicone oil that results in the transition from liquid to solid. Double-19 and RTV-A are two kinds of vinyl silicone oils, their vinyl content and degree of polymerization are different, and

there is a certain trade-off between the polymerization rate and physical strength. The hydrogen silicone oil RTV-B can automatically crosslink with the vinyl silicone oil under the action of a platinum catalyst to realize a rapid liquid–solid phase transition. Since the polymerization of this mixture does not require other inducers such as ultraviolet light at the beginning, it minimizes the damage to biological materials (cells and nucleic acids), reduces the requirement for equipment and is user-friendly. The curing times of fresh oil were 280 min, 37 min and 1.1 min at 25, 37, and 95 °C, respectively, as shown in Fig. 3A. The characteristics of the slow reaction at 25 °C and fast transformation at 37 °C give this water-immiscible liquid advantages of a broad operation window and a short lag time of monitoring.

Fig. 3B shows that the thermosetting oil can generate uniform sized droplets. The medium diameter of the droplets was 49.7 μm with a coefficient of variation (CV) of 3.7% (Fig. 3C). Meanwhile, droplet stabilization is necessary for bacterial growth. When there are no cells in the droplet, the droplet can maintain good stability. Different from empty droplets, when bacteria are cultured in them, due to cell metabolism, the substance concentration in the droplet containing cells changes with incubation time, resulting in different osmotic pressures between droplets. Then, the diaphragm, that is, the solidified thermosetting oil with nano-channels between adjacent droplets, is used as a dialysis membrane to allow water to transfer freely between the droplets with different osmotic pressures and deform or even rupture.[41] Therefore, we determine the stability of the thermally solidified droplets by observing the migration of fluo-
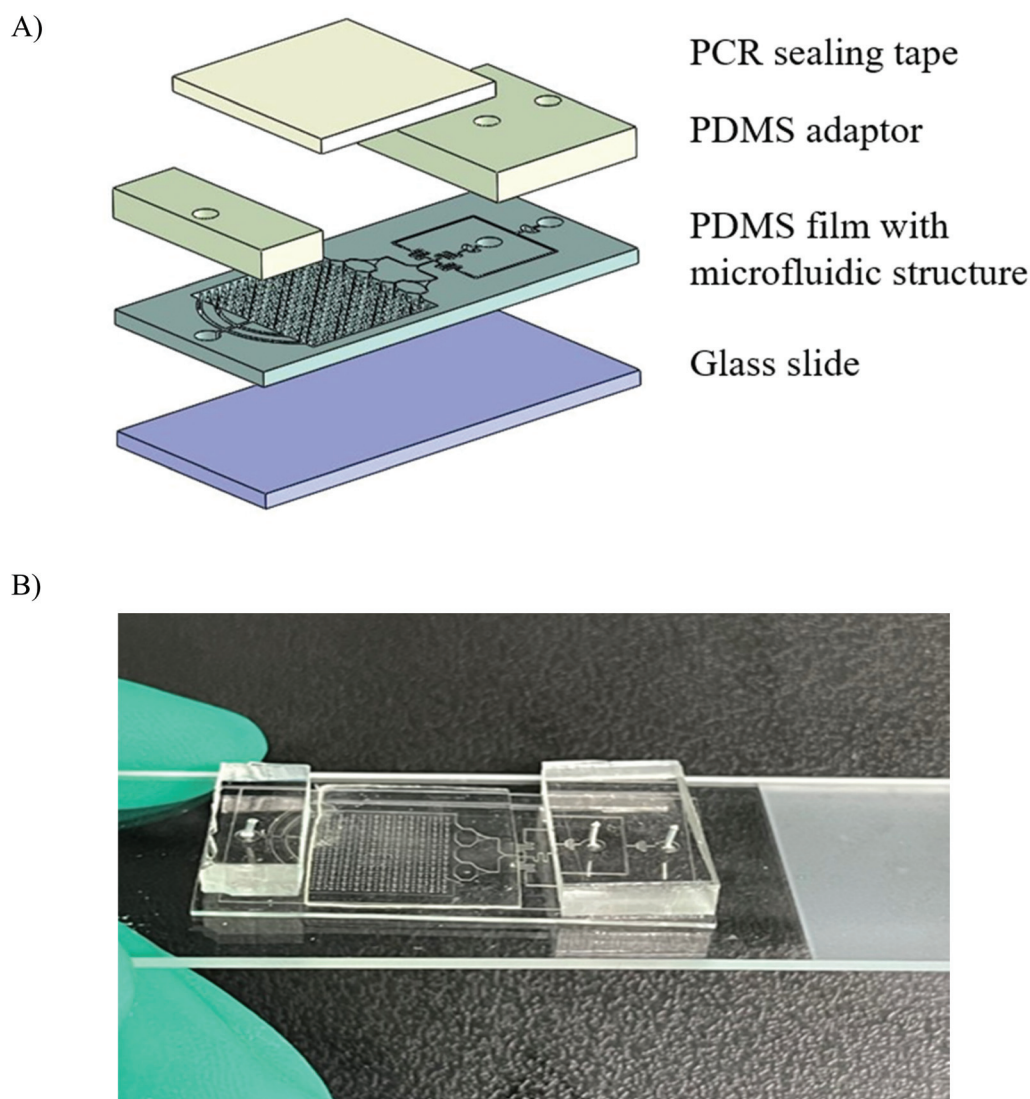
Fig. 2 (A) Diagram of the layered device structure of the microfluidic chip. (B) Photo of the microfluidic chip.

rescence in the droplets under a fluorescence microscope. After droplet generation, the sealed microfluidic chip was incubated at 37 °C and photographed at 2, 4, 6 and 18 hours to determine the percentage of intact droplets. As shown in Fig. 3D, the droplets can maintain more than 90% integrity within 6 hours at 37 °C, with the value of 97.2% at 2 h, 95.7% at 4 h, and 94.7% at 6 h and even 87.4% at 18 h. These results show that the thermosetting droplets have good stability within 6 hours, and there are fewer damaged droplets with the extension of culture time. At the same time, after the droplet solidifies, the position of the droplet remains unchanged, which makes it possible to track the growth of a single cell. In addition, we observed a phenomenon in the experiment that with the extension of the droplet culture time, black substances will precipitate in the droplet. This is probably caused by the substances metabolized by *E. coli* during their growth. Through continuous

observation, the precipitated black matter does not affect the stability of the droplets and the growth of *E. coli*.

3.3. Single cell encapsulation of bacteria in pico droplets

Single *E. coli* cells are reliably stochastically confined, cultivated, and detected *via* fluorescence in our pico-droplet array. The distribution of every single cell is random and independent. The number of cells in every droplet is also random and independent. Therefore, Poisson distribution is used to estimate the number of cells per droplet including the probability associated (eqn (1)). Table S1† shows the percentages of droplets (∼60 pL) with 0, 1 or 2 cells. When the concentration was lower than 10^6 CFU mL^{-1}, we could make sure about 99.85% droplets contain one or zero cell. Even when the concentration was 10^7 CFU mL^{-1}, the percentage of droplets with one or zero cell was still about 88%. So, when the concentration of the sample was less than 10^7 CFU mL^{-1}, we could make sure the
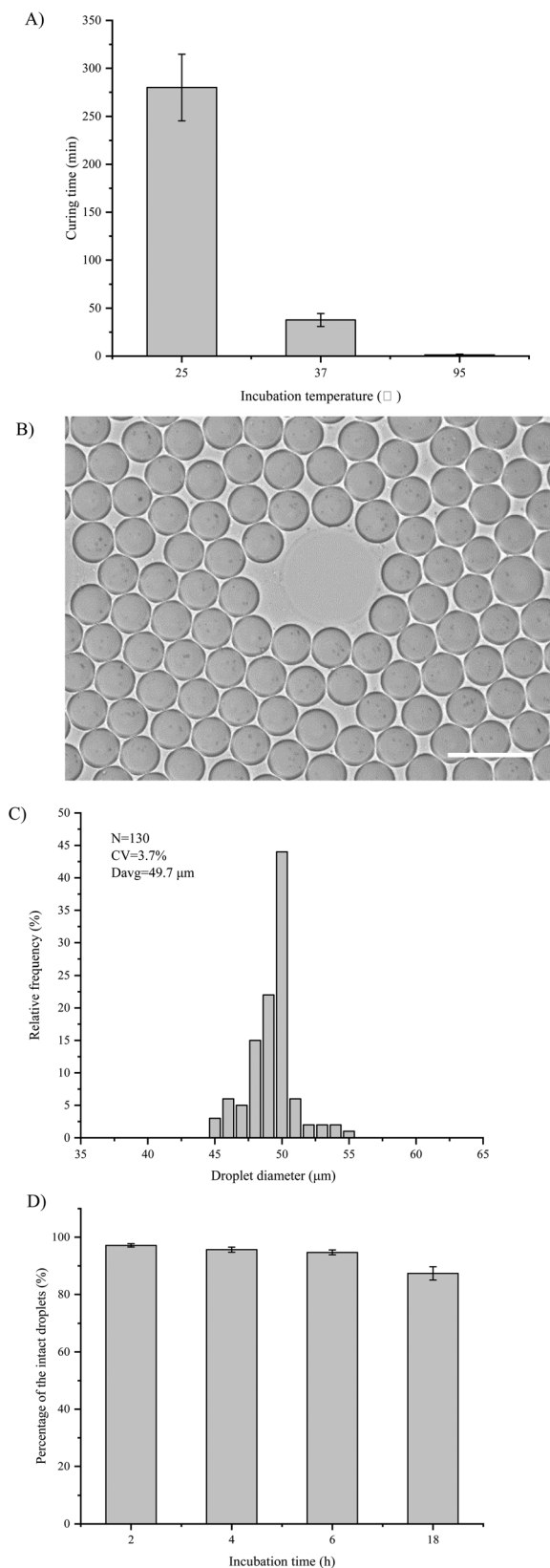
Fig. 3 (A) Curing time of the thermosetting oil at different temperatures. (B) Monodisperse droplets generated in the thermosetting oil at 0 h. (C) Size distribution of the droplets. (D) Percentage of the intact droplets over time. Scale bar is 100 μm.

ratio of a droplet with multiple cells was less than 10%. The result showed that the ratio of droplets with multi-cell occupancy was statistically insignificant and could be neglected for quantifying samples with the bacterial density ranging from 10^2 to 10^7 CFU mL^{-1}. In order to achieve cell monodispersion, the value of λ should usually be controlled below 0.2, so as to achieve better monodispersion.[42] In this study, we have achieved a λ value below 0.2 at the input concentration of 10^5 CFU mL^{-1}. Similar to the droplet digital PCR technology, in our experiment, we used resazurin as a fluorescent dye to amplify the bacterial growth signal through the fluorescent signal. After droplet generation and solidification, *E. coli* cells were dispersed in droplets, each containing one or no cells. With the proliferation of bacterial cells, resazurin was reduced to resorufin, exhibiting strong fluorescence characteristics. Thus, the positive (fluorescent) droplets are considered to be the result of the proliferation of a single bacterium. The viable bacteria amount can be obtained by counting the number of positive droplets. The detailed calculation method is shown in the ESI.†

$$P(x = k) = \frac{e^{-\lambda}}{k!}\lambda^k \qquad (1)$$

$$\lambda = C \cdot V \qquad (2)$$

Thus,

$$\text{bacteria concentration} = -\frac{\ln\left(1 - \dfrac{\text{positive}}{\text{total}}\right)}{V}$$

In Eqn (1), P($x = k$) is the probability to have k cells per droplet and λ is the mean number of cells per droplet. In Eqn (2), C represents the concentration of bacterial cells and V is the average volume per pico-droplet.

3.4. Dynamic fluorescence detection and tracking of bacteria in pico droplets

Our strategy for viable bacteria counting was to take advantage of the proliferation of individual cells in individual droplets, reducing non-fluorescent resazurin to fluorescent resorufin, so that the number of viable bacteria was finally inferred by counting the fluorescently positive droplets. To demonstrate, we injected previously quantified *E. coli* suspensions ranging from 2×10^7 CFU mL^{-1} to 2×10^2 CFU mL^{-1} into our device. We incubated the pico-droplet array at 37 °C for 5 h. Fluorescence images and bright field images were taken every hour. We used a 10^6 CFU mL^{-1} bacterial solution to determine the incubation time. We found that positive droplets could be better distinguished from negative ones at the fourth hour, as shown in Fig. 4A. Therefore, we recommend 4 h as the incubation time for droplets. Then the final concentration of *E. coli* from the samples was calculated according to Poisson distribution. Each sample was measured at least three times and a part of the fluorescent images is shown in Fig. 4B to establish a calibration curve for the detection of *E. coli*. It clearly shows a positive correlation between bacterial concentration and the number of fluorescently positive droplets. In addition, we
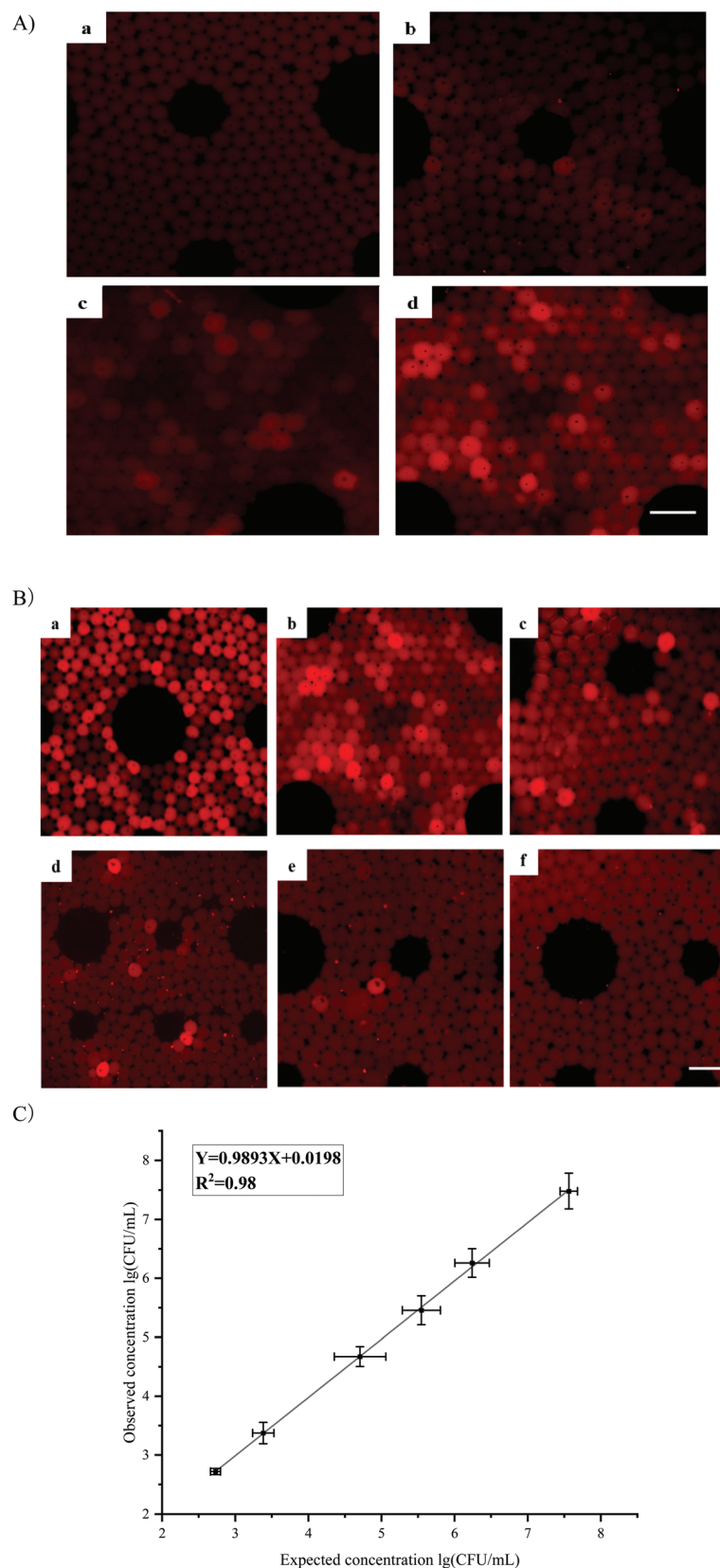
Fig. 4 (A) Fluorescence images of droplets after incubation for 1 h to 4 h with the concentration of 10^6 CFU mL^{-1}: (a) 1 h, (b) 2 h, (c) 3 h, and (d) 4 h. (B) Typical fluorescence images corresponding to different concentrations of *E. coli* at 4 h: (a) 10^7 CFU mL^{-1}, (b) 10^6 CFU mL^{-1}, (c) 10^5 CFU mL^{-1}, (d) 10^4 CFU mL^{-1}, (e) 10^3 CFU mL^{-1} and (f) 500 CFU mL^{-1}. (C) The linear correlation between the observed and expected values. Scale bar is 100 μm.
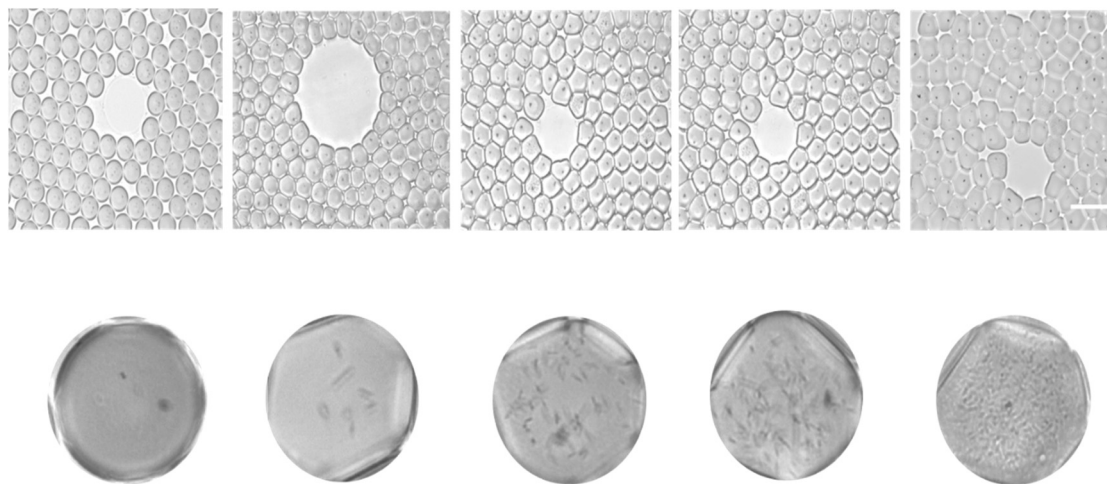
Fig. 5 Real-time monitoring of the growth of single *E. coli* cells from 0 h to 4 h. Scale bar is 100 μm.

investigated the relationship between the actual concentration of the sample (plate counting method; expected value) and the concentration derived from the digital counting method (observed value). There is a good linear correlation ($R^2 = 0.989$) between the observed values and the expected values (Fig. 4C), indicating the satisfactory performance of the thermosetting droplets for digital counting.

Because our pico-droplet array was solidified, we also tracked the proliferation of *E. coli* cells within individual droplets. As shown in Fig. 5, the droplets dispersed by a single *E. coli* cell were difficult to separate from the negative droplets when the droplet array was just formed. Then, as the incubation time increased, the density of the positive droplets increased significantly higher than that of the negative droplets. Many swimming rod-shaped *E. coli* cells could be observed in the positive droplets. The results above show that the thermally solidified droplets are easy to track the dynamic signal changes in a single droplet. Compared with other literature reports,[43,44] the droplets produced by our method are relatively fixed, and the size and the number of droplets are flexible and thus they can provide information on the dynamics of individual droplets. Our method can also be used to monitor the susceptibility of single cells to drugs in real-time by immobilizing single droplets in the future.

3.5. Real sample detection

Milk samples were used to verify the feasibility of the method while dealing with real samples. We dispersed unknown concentrations of *E. coli* cells into milk and used both plate counting and droplet array methods to unambiguously determine bacterial concentrations. The results are shown in Fig. 6. Both the plate count method and thermosetting droplet methods allow bacterial concentrations to be calculated, but the droplet method greatly saves incubation time.

4. Conclusion

In summary, we successfully generated a pico-liter scale droplet array and achieved droplet immobilization at culture temperature by using a cross-linking reaction of the thermosetting oil. In the presence of the Pt catalyst, the solidification of mixed oil starts spontaneously without inducers, such as UV and charged icons, avoiding the damage of bacterial cells by the inducers. *E. coli* cells and their cultures were dispersed in thermosetting droplets and high-throughput monodisperse droplets provided *E. coli* cells with an isolated environment for single cell tracking and culturing. The growth signal of bacteria in droplets is converted to a fluorescent signal by an indicator, so that digital counting of bacteria can be achieved by counting positive droplets. We have accelerated the detection of microcolonies that have replicated from single bacteria in

Fig. 6 Counting results of *E. coli* cells in milk samples by plate counting and droplet counting methods.

4 h and have a detection limit for viable *E. coli* of 500 CFU mL^{-1}. Compared with the conventional plate counting method, our method greatly reduces the detection time, and at the same time, the digital counting results are consistent with those of the plate method. In addition, because of the solidified nature of droplets, we also monitored the proliferation of a single bacterium in the droplets in real time to ensure normal bacterial growth. It can be found that with the extension of incubation time, the density of bacteria in the droplet increases, thus forming a microcolony. Our method provides a new strategy for food pathogenic bacteria detection. Our method also provides a new way to study cell growth dynamics. Our method can be further used to observe bacterial resistance as well as some other responses in future.

Author contributions

Yuanjie Suo: Conceptualization, methodology, visualization, writing – original draft, and writing – review and editing. Weihong Yin: Methodology. Wenshuai Wu: Writing – review and editing. Qiangyuan Zhu: Writing – review and editing. Wenjian Cao: Writing – review and editing. Ying Mu: Writing – review and editing and funding acquisition.

Conflicts of interest

The authors declare that they have no known competing financial interests or personal relationships that could have appeared to influence the work reported in this paper.

Acknowledgements

References

1 J. M. Choi, E. Camfield, A. Bowman, K. Rajan, N. Labbe, K. D. Gwinn, B. H. Ownley, N. Moustaid-Moussa and D. H. D'Souza, *Food Microbiol.*, 2021, **95**, 103674–103674.

2 F. Dell'Orco, C. Gusmara, M. Loiacono, T. Gugliotta, F. Albonico, M. Mortarino and A. Zecconi, *Res. Vet. Sci.*, 2019, **123**, 77–83.

3 X. Hu, Y. Li, Y. Xu, Z. Gan, X. Zou, J. Shi, X. Huang, Z. Li and Y. Li, *Food Chem.*, 2021, **339**, 127775.

4 N. Dhull, G. Kaur, P. Jain, P. Mishra, D. Singh, L. Ganju, V. Gupta and M. Tomar, *Appl. Surf. Sci.*, 2019, **495**, 7.

5 A. Townsend, S. Li, D. A. Mann and X. Deng, *Food Microbiol.*, 2020, **92**, 103575.

6 D. Kaye, *Clin. Infect. Dis.*, 2018, **67**, I–II.

7 L. Lin, X. L. Wang, C. Z. Li and H. Y. Cu, *Ultrason. Sonochem.*, 2019, **59**, 10.

8 D. Rodriguez-Lazaro, B. Lombard, H. Smith, A. Rzezutka, M. D'Agostino, R. Helmuth, A. Schroeter, B. Malorny, A. Miko, B. Guerra, J. Davison, A. Kobilinsky, M. Hernandez, Y. Bertheau and N. Cook, *Trends Food Sci. Technol.*, 2007, **18**, 306–319.

9 J. Choi, J. Lee and J. H. Jung, *Biosens. Bioelectron.*, 2020, **169**, 112611.

10 H. H. Li, W. Ahmad, Y. W. Rong, Q. S. Chen, M. Zuo, Q. Ouyang and Z. M. Guo, *Food Control*, 2020, **107**, 8.

11 R. D. Hoelzle, B. Virdis and D. J. Batstone, *Biotechnol. Bioeng.*, 2014, **111**, 2139–2154.

12 C. Davis, *J. Microbiol. Methods*, 2014, **103**, 9–17.

13 T. S. Kaminski, O. Scheler and P. Garstecki, *Lab Chip*, 2016, **16**, 2168–2187.

14 A. D. Griffiths and D. S. Tawfik, *Trends Biotechnol.*, 2006, **24**, 395–402.

15 Y. Ding, P. D. Howes and A. J. deMello, *Anal. Chem.*, 2020, **92**, 132–149.

16 J. Q. Boedicker, L. Li, T. R. Kline and R. F. Ismagilov, *Lab Chip*, 2008, **8**, 1265–1272.

17 M. E. Vincent, W. S. Liu, E. B. Haney and R. F. Ismagilov, *Chem. Soc. Rev.*, 2010, **39**, 974–984.

18 X. J. Bian, F. X. Jing, G. Li, X. Y. Fan, C. P. Jia, H. B. Zhou, Q. H. Jin and J. L. Zhao, *Biosens. Bioelectron.*, 2015, **74**, 770–777.

19 E. Hondroulis, A. Movila, P. Sabhachandani, S. Sarkar, N. Cohen, T. Kawai and T. Konry, *Biotechnol. Bioeng.*, 2017, **114**, 705–709.

20 C. N. Baroud, F. Gallaire and R. Dangla, *Lab Chip*, 2010, **10**, 2032–2045.

21 A. P. Debon, R. C. R. Wootton and K. S. Elvira, *Biomicrofluidics*, 2015, **9**, 024119.

22 R. R. Pompano, W. Liu, W. Du and R. F. Ismagilov, in *Annual Review of Analytical Chemistry*, ed. R. G. Cooks and E. S. Yeung, 2011, vol. 4, pp. 59–81.

23 Q. Zhong, S. Bhattacharya, S. Kotsopoulos, J. Olson, V. Taly, A. D. Griffiths, D. R. Link and J. W. Larson, *Lab Chip*, 2011, **11**, 2167–2174.

24 Y. D. Ma, K. Luo, W. H. Chang and G. B. Lee, *Lab Chip*, 2018, **18**, 296–303.

25 A. Huebner, D. Bratton, G. Whyte, M. Yang, A. J. deMello, C. Abell and F. Hollfelder, *Lab Chip*, 2009, **9**, 692–698.

26 L. Labanieh, T. N. Nguyen, W. Zhao and D.-K. Kang, *Micromachines*, 2015, **6**, 1469–1482.

27 N. Shembekar, H. Hu, D. Eustace and C. A. Merten, *Cell Rep.*, 2018, **22**, 2206–2215.

28 S. Sarkar, P. Sabhachandani, D. Stroopinsky, K. Palmer, N. Cohen, J. Rosenblatt, D. Avigan and T. Konry, *Biomicrofluidics*, 2016, **10**, 054115.

29 C. H. J. Schmitz, A. C. Rowat, S. Koester and D. A. Weitz, *Lab Chip*, 2009, **9**, 44–49.

30 W. Wu, S. Zhou, J. Hu, G. Wang, X. Ding, T. Gou, J. Sun, T. Zhang and Y. Mu, *Adv. Funct. Mater.*, 2018, **28**, 1803559.

31 Y. He, J. X. Yin, W. S. Wu, H. X. Liang, F. T. C. Zhu, Y. Mu, H. L. Fan and T. Zhang, *Anal. Chem.*, 2020, **92**, 8530–8535.

32 W. H. Tan and S. Takeuchi, *Adv. Mater.*, 2007, **19**, 2696.

33 J. L. Chen, R. Ortiz, Y. Y. Xiao, T. W. J. Steele and D. C. Stuckey, *Water Res.*, 2015, **75**, 123–130.

34 M. Azizi, M. Zaferani, B. Dogan, S. Y. Zhang, K. W. Simpson and A. Abbaspourrad, *Anal. Chem.*, 2018, **90**, 14137–14144.

35 L. Liu and S. Choi, *Lab Chip*, 2017, **17**, 3817–3825.

36 F. Liebisch, A. Weltin, J. Marzioch, G. A. Urban and J. Kieninger, *Sens. Actuators, B*, 2020, **322**, 8.

37 L. Cao, X. Cui, J. Hu, Z. Li, J. R. Choi, Q. Yang, M. Lin, H. Ying and F. Xu, *Biosens. Bioelectron.*, 2017, **90**, 459–474.

38 Q. Song, Y. B. Gao, Q. Y. Zhu, Q. C. Tian, B. W. Yu, B. F. Song, Y. N. Xu, M. K. Yuan, C. C. Ma, W. Jin, T. Zhang, Y. Mu and Q. H. Jin, *Biomed. Microdevices*, 2015, **17**, 8.

39 K. A. Heyries, C. Tropini, M. VanInsberghe, C. Doolin, O. I. Petriv, A. Singhal, K. Leung, C. B. Hughesman and C. L. Hansen, *Nat. Methods*, 2011, **8**, 649–U664.

40 Q. Y. Zhu, L. Qiu, B. W. Yu, Y. N. Xu, Y. B. Gao, T. T. Pan, Q. C. Tian, Q. Song, W. Jin, Q. H. Jin and Y. Mu, *Lab Chip*, 2014, **14**, 1176–1185.

41 W. S. Wu, S. Zhang, T. Zhang and Y. Mu, *ACS Appl. Mater. Interfaces*, 2021, **13**, 6081–6090.

42 K. Hsieh, H. C. Zec, L. B. Chen, A. M. Kaushik, K. E. Mach, J. C. Liao and T. H. Wang, *Anal. Chem.*, 2018, **90**, 9449–9456.

43 X. S. An, P. Zuo and B. C. Ye, *Talanta*, 2020, **209**, 120571.

44 S. D. Brugger, C. Baumberger, M. Jost, W. Jenni, U. Brugger and K. Muhlemann, *PLoS One*, 2012, **7**, 6.